

A new experimental test of the usefulness of Burnett-Type corrections for the viscosity of a gas

M. García-Sucre^{1*}, G. Urbina-Villalba¹, L.A. Araque-Lamedá² and R.E. Parra¹

¹ Centro de Física, Instituto Venezolano de Investigaciones Científicas (IVIC)
Apartado 21827. Caracas 1020 A, Venezuela

² Departamento de Física, Escuela de Ciencias, Núcleo de Sucre, Universidad de Oriente
Cumaná, Venezuela

Recibido: 26-06-96 Aceptado: 29-11-96

Abstract

The effective viscosity of a helium gas in the transition regime has been measured with an improved version of a torsion pendulum viscometer with thermally controlled walls. The experimental results have been analyzed in terms of a model including Burnett-type corrections that takes into account the cylindrical geometry of the system. Our results bring an additional indication of the importance of Burnett-type corrections to that recently found by Salomons and Mareschal in the quite different problem of atomistic simulations of a strong shock wave in a hard-sphere gas.

Key words: Burnett-corrections; transition regime; viscosity.

Nuevos resultados experimentales sobre la utilidad de las correcciones tipo Burnett para la viscosidad de un gas

Resumen

La viscosidad efectiva de un gas de helio en el régimen de transición es medida con una versión de un viscosímetro de péndulo de torsión con las paredes externas a temperatura controlada. Los resultados experimentales han sido analizados en términos de un modelo que incluye correcciones tipo Burnett y que a la vez toma en cuenta la geometría cilíndrica del sistema. Nuestros resultados muestran la importancia que pueden tener las correcciones tipo Burnett, importancia que ha sido también ilustrada por los resultados de Salomons y Mareschal en simulaciones numéricas de una onda de choque en un gas de esferas rígidas.

Palabras claves: Correcciones de Burnett; régimen de transición; viscosidad.

Introduction

Starting from the Boltzmann equation it can be shown that for a dilute gas there are additional terms to those corresponding to the Newton law of friction and the Fourier law of heat conduction (1):

$$P_{zx} = -\eta \frac{\partial u_x}{\partial z} + (P_{zx})_B \quad [1]$$

and

$$J_z = -\kappa \frac{\partial T}{\partial z} + (J_z)_B \quad [2]$$

* To whom correspondence should be addressed.

where $(P_{zx})_B$ and $(J_z)_B$ stand for the above mentioned additional terms, and η and κ are the usual coefficients of viscosity and thermal conductivity. Both $(P_{zx})_B$ and $(J_z)_B$ consist of a series of terms each of which are the product of a coefficient (depending on thermodynamic variables and molecular parameters), and either the product of gradients or high order derivatives of u_x and/or T . We will call $(P_{zx})_B$ and $(J_z)_B$ Burnett type corrections because of the Burnett equations as a generalization of the Navier-Stokes equations (2,3).

The terms appearing in $(P_{zx})_B$ and $(J_z)_B$ may become relevant in at least two situations:

(i) When the Match number M is large (M is the ratio of the fluid velocity and the velocity of sound). In that case, due to the relatively large value of the fluid velocity, high order derivatives and non-linear fluid velocity gradient factors in terms of $(P_{zx})_B$ and $(J_z)_B$ may take values making relevant these corrections (3).

(ii) When the mean free path l cannot be neglected in front of a characteristic macroscopic length L of the system under consideration. In that case the coefficients of the terms appearing in $(P_{zx})_B$ or $(J_z)_B$ are large due to their dependence on $(l/L)^n$ ($n \geq 2$) (4,5).

Recently it has been shown using atomic simulations for a strong shock wave in a hard-sphere gas that the Burnett type corrections considerably improve the description of the thermal conductivity and the viscosity over the Navier-Stokes predictions in the shock-front region (3). This clearly indicates the importance of additional terms appearing in $(P_{zx})_B$ and $(J_z)_B$ for the first of the two types of situations above mentioned.

Here, we will examine situation (ii). For this we will consider the experimental measurement of the effective viscosity as a function of the density of a gas confined to a cylindrical container, inside which a torsion

pendulum consisting of a cylindrical moving shell hangs suspended from a quartz fiber.

The experiment has the following general characteristics:

a) The tangential velocity of the moving shell is sufficiently small so that in our experiment the Match number is much smaller than unity.

b) The parameters characterizing our system are such that the correspondent Reynold number is found in a range of values very far from that corresponding to the occurrence of turbulence.

c) The pressure and temperature of the gas correspond to the so called transition regime case ($l \sim L$).

The theoretical model that we will use to interpret our experimental results includes additional terms in $(P_{zx})_B$. Equation [1], up to third order in l and consider explicitly a cylindrical geometry. A condensed description of it will be given in section 2. A more complete account of this model is given in Reference 6.

An intuitive description of the physics behind of the unusual oscillations of viscosity in the transition regime is given in Reference 7.

We will concentrate here on the prediction of this model according to which the effective viscosity in the transition regime presents periodic regions of rapid variation as a function of density; the separation in density Δn between these regions fulfilling the simple equation:

$$\Delta n = \frac{1}{\left(\frac{4}{3\pi^3}\right)^{1/2} \Delta R \sigma} \quad [3]$$

where σ is the mean atomic cross-section of the gas and ΔR the radial separation between concentric surfaces which are in relative motion.

Here we report experimental results for the effective viscosity of helium in the transition regime (section 3). These results strongly depart from what is expected when $(P_{zz})_B$ is neglected in Equation [1]. The experimental measurement of effective viscosity shows regions of rapid variation with the density and the location in density of these regions can be reasonably well described by Equation [3]. The experimental results have been obtained with an improved version of a viscometer corresponding to $\Delta R = 2.0 \pm 0.1$ cm. The comparison of these results with those previously reported by us for helium employing a viscometer with $\Delta R = 5.0 \pm 0.1$ cm (5), indicates that the relation $\Delta n \propto 1/\Delta R$ that follows from Equation (3) holds. Finally the present results are also contrasted with those previously obtained with a third viscometer whose moving shell is not equidistant from the two fixed surfaces of the apparatus (8).

Viscosity of a gas in the transition regime and in a centrifuge field of force

Let us consider a dilute gas, enclosed in a cylindrical recipient of radius R , which rotates around the symmetry axis with constant angular velocity $\vec{\Omega}$. To describe this system we use two cylindrical coordinate systems: one fixed in the laboratory, and the other rotating with angular velocity $\vec{\Omega}$, but having the same origin and the same Z axis as the fixed system. We denote \vec{U} , the thermal velocity of a molecule measured in the rotating coordinate system, and \vec{V} the velocity of the same molecule measured in the fixed coordinate system. Using cylindrical coordinates ρ, ϕ and Z , the local distribution function can be written as (6)

$$f^{(0)}(\rho, \vec{U}) = n(\rho) \left[\frac{m}{2\pi kT} \right]^{3/2} \exp \left[-\frac{mU^2}{2kT} \right], \quad [4]$$

where k is Boltzmann's constant, $\vec{U} = (U_\rho, U_\phi, U_z)$, $U_\rho = v_\rho$, $U_\phi = v_\phi - u_\phi(\rho)$, $U_z = v_z$, and $u_\phi(\rho)$ is the fluid velocity. The local density $n(\rho)$ depends on the radial variable ρ . In fact, it can be shown to depend very weakly on ρ except when very high angular velocities occur, which is not the case of our experiments here (6).

Following the path integral method, the molecular distribution function can be calculated up to third order in the mean collision time τ (4-6). Using this molecular distribution function f and following a similar procedure to that previously described (6), the tangential stress $P_{\rho\phi} = m \int d^3U f U_\rho U_\phi$, is found to be (6):

$$P_{\rho\phi} = nkT\tau \frac{\partial U_\phi}{\partial \rho} - 3\tau^3 \frac{k^2 T^2}{m} \left[2 \frac{\partial^2 n}{\partial \rho^2} - \frac{3}{n} \left(\frac{\partial n}{\partial \rho} \right)^2 \right] \frac{\partial U_\phi}{\partial \rho} - 3n\tau^3 \frac{k^2 T^2}{m} \frac{\partial^3 U_\phi}{\partial \rho^3} \quad [5]$$

where the last two terms in the r.h.s. correspond to third order Burnett-type corrections in the collision time. We will ignore in Eq [5] the terms arising because of the dependence of n on ρ .

The problem of the boundary conditions for Equation [5] was already considered in Reference 6. The nature of the interaction between the molecules of the gas and the solid surfaces is a complex problem depending on the physical and chemical properties of the surfaces and on the molecules of the gas. We have taken into account this complexity in an effective way through the values that the fluid velocity and the spatial derivative of it may take in the neighborhood of the solid surfaces. For instance, at the most elementary level we may consider the slipping factors of the gas at this surface in an effective way, when the value v_1 of v_ϕ at $\rho = R_1$ is smaller than the tangential velocity of the solid surface corresponding to $\rho = R_1$. The effect of the boundary conditions on viscosity has been already

studied for a variety of cases. As was previously shown, the periodic non monotonic variation of the viscosity with density remains even under random values of the derivative of the fluid velocity at the container walls (6).

For the boundary conditions

$$v_1 = v_\phi(\rho = R_1), \quad v_2 = v_\phi(\rho = R_2),$$

$$a_1 = \frac{\partial v_\phi}{\partial \rho} \Big|_{\rho = R_1}, \quad \text{and} \quad a_2 = \frac{\partial v_\phi}{\partial \rho} \Big|_{\rho = R_2}$$

where $\rho=R_1$ and $\rho=R_2$ correspond to the fixed and the moving surfaces of the viscometer, respectively, along with a condition of zero relative acceleration of the concentric layers:

$$2\pi H \rho P_{\rho\phi} = \text{const},$$

Equation [5], yields (6):

$$P_{R_2\phi} = -\eta_0 \left\{ \frac{1 - \frac{a_1 + a_2}{\omega \Delta v} \tan \frac{\omega \Delta R}{2}}{g_2 - g_1 + 1 + n(R_2/R_1) - (f_1 + f_2) \tan \left(\frac{\omega \Delta R}{2} \right) \frac{R_2}{\Delta R}} \right\} \frac{\Delta v}{\Delta R} \quad [6]$$

where $\omega = (\pi/3\tau^2\kappa T)^{1/2} \equiv (8/3\pi)^{1/2} \sqrt{2} \sigma n$, $\Delta v = v_2 - v_1$, $\Delta R = R_2 - R_1$, and

$$g(R) = \frac{\pi}{2} \text{sen} \omega R - CI(\omega R) \cos \omega R - SI(\omega R) \text{sen} \omega R, \quad [7]$$

$$f(R) = \frac{\pi}{2} \cos \omega R + CI(\omega R) \sin \omega R - SI(\omega R) \cos \omega R, \quad [8]$$

$g_1 \equiv g(R_1)$, $g_2 \equiv g(R_2)$, $f_1 \equiv f(R_1)$, $f_2 \equiv f(R_2)$, and $SI(x)$ and $CI(x)$ are the well known integral functions (9). It can be shown that the limit $R_1, R_2 \rightarrow \infty$ of $P_{\rho\phi}$ given in Equation [6] with $\Delta R = L = \text{constant}$, leads to the expression of the stress tensor corresponding to a planar geometry given in Equation [41] of Reference 5. On the other hand, the high density limit of Equation [6] gives the correct continuous regime expression. The stress-

tensor component $P_{\rho\phi}$ given by Equation [6] predicts regions of rapid variation with density which are separated by the quantity Δn given in Equation [3]. Finally, although Equation [6] yields values for the effective viscosity which may differ in a sizable way from the corresponding ones obtained previously for a planar geometry (5), the expression for Δn is the same for the two cases (5). This is relevant to our discussion of the experimental results in the next sections.

Experimental

Figures 1 and 2 show a simplified scheme of the viscometer used. The main characteristics of this instrument are:

i) Hollow fix walls (Figure 1) were built, and a couple of thermostated baths has been attached to each of the walls in order to keep the temperature gradient constant; ii) Two platinum resistance sensors has been placed near the fix and moving walls in order to monitor temperature variations; iii) A pressure sensor system which includes a digital Pirani-PG3 vacuum gauge, as well as a sensitive thermal conductivity gauge heads was added (Figure 2); iv) A stepping motor has been attached to the precision rotatory feed through with the aid of a rubber band (Figure 2) in order to transmit similar torques to the torsion pendulum as the experiment evolves. This device greatly diminishes the human error, lowering any influence of the initial torque in the resulting oscillations. In all cases, the stepping motor controller has been turned off after the appropriate torque was given in order to avoid the transmission of unwanted vibrations to the viscometer.; v) The output of the laser phototransistor has been connected to a personal computer with the use of a multifunction analog/digital board and appropriate termination breadboards (Figure 2).

A C-coded program elaborated with LabWindows (version 2.2) and the addition of a AT-MIO-16H-25 card to a PC, has allowed to record the pressure, temperature

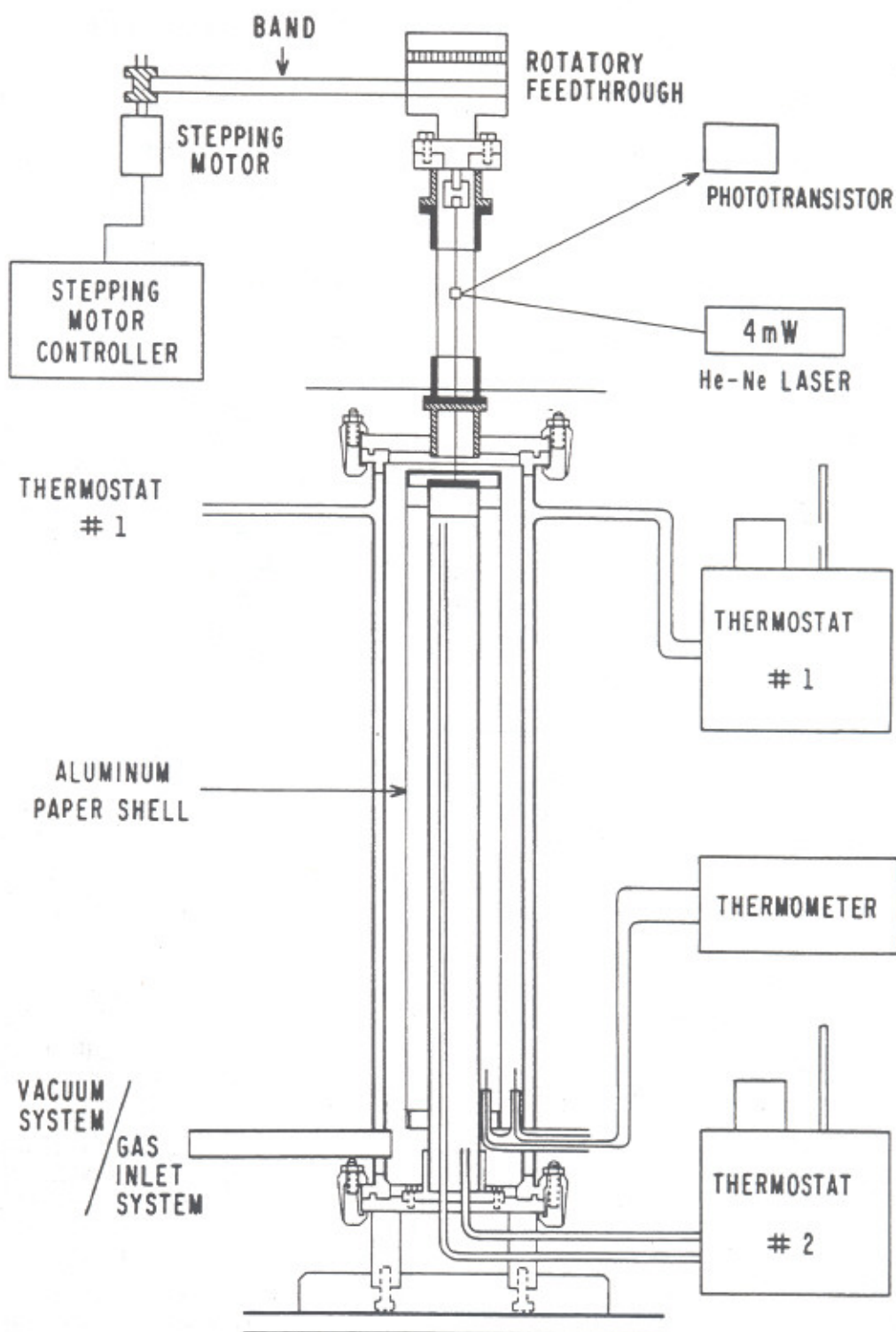


Figure 1. Torsion pendulum viscometer with thermally controlled walls.

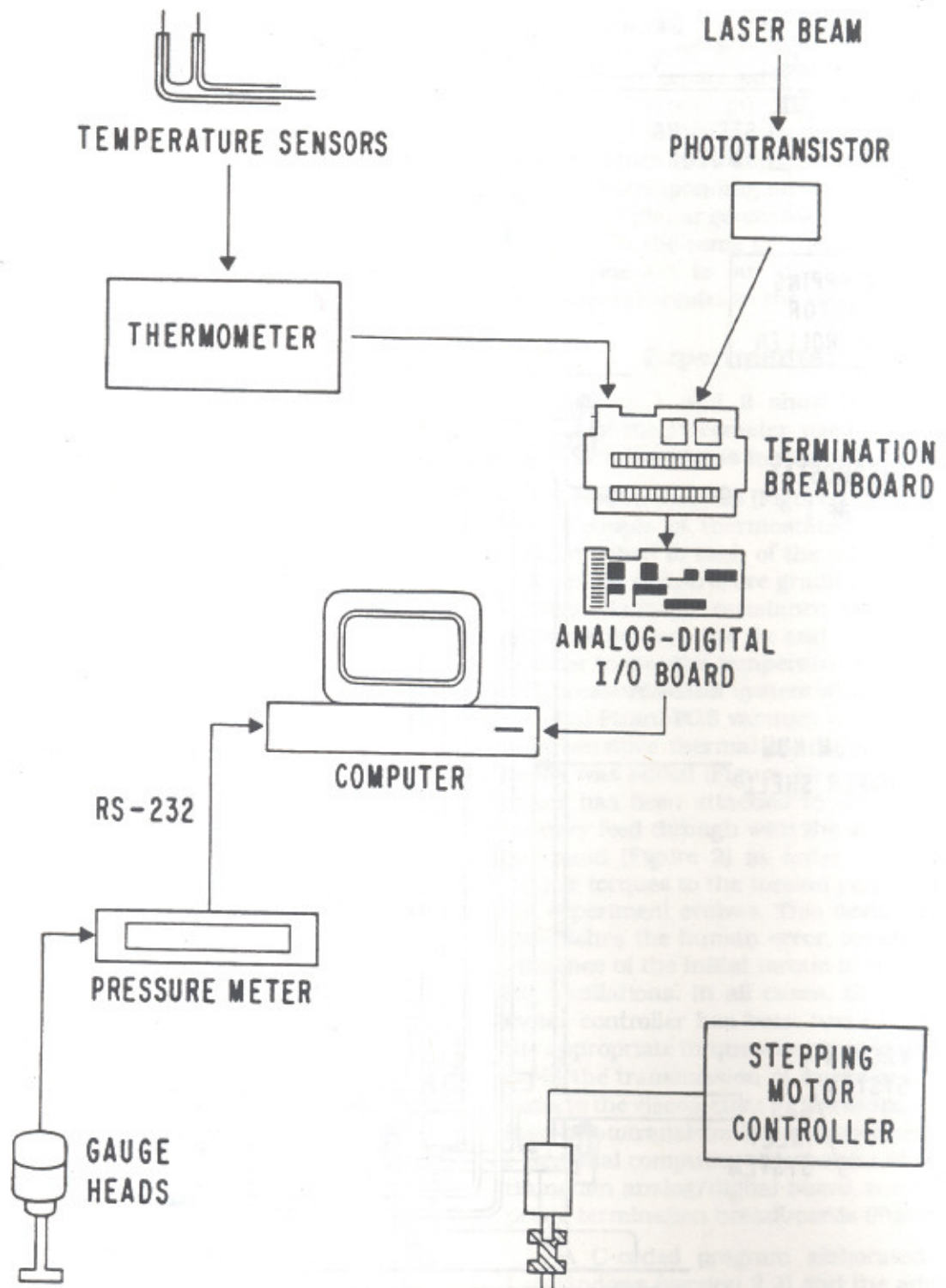


Figure 2. Scheme of the measurement system of the viscometer and data processing devices.

and elapsed time at each laser pulse detected by the phototransistor. In this way, all relevant data can be recorded for each period of oscillation, allowing separate analysis of their variation with respect to the pressure.

A cylindrical aluminum paper moving shell weighing 52.8 ± 0.1 g. and having a total length of 70.0 ± 0.1 cm., was employed. A distance of 2.00 ± 0.05 cm. between the fix and moving walls was selected (ΔR). Fifteen degrees torques were used in order to impulse the pendulum. The periods of oscillation were recorded within an angle of 15 degrees from the equilibrium point. The pressure was changed from 1 to 50 $\mu\text{m Hg}$ in approximately 1.5 $\mu\text{m Hg}$ steps, and some other points were taken in order to reach 150 $\mu\text{m Hg}$. It has been found convenient to start from the highest pressure and lower the pressure gradually, since in that way the pressure is much more easily controlled. The temperature was held constant at 293 K, with maximum deviations of less than 0.2 K. The accuracy of the time counter is the order of 10^{-5} seconds, being the average period of oscillation of the viscometer about 23.05 seconds for the range of selected pressures.

Using the dependence of the periods of oscillations with the pressure (4), a cubic spline fit of the variation of $f = -P_{\text{eff}} \Delta R / \eta_0 \Delta v$ was drawn (Figure 3). The function f can be written as (4):

$$f = \frac{4\pi M \Delta R}{\eta_0 A} \frac{(T_i^2 - T_0^2)^{1/2}}{T_i T_0}, \quad [9]$$

where T_i is the experimental value of the period of oscillation of the torsion pendulum corresponding to the pressure p_i . The quantities M and A are the mass and the area of the moving shell of the torsion pendulum, and η_0 is the viscosity of the gas in the continuous regime. We have given to T_0 in Equation [9] the value of the minimum of the measured periods T_i 's in each experiment corresponding to a run in the pressu-

re. Each point in Figure 3 corresponds to the average period of oscillation of a set of 11 periods recorded at each pressure. This figure shows an upward drift on top of which the oscillations are clearly seen. This drift depends on the gas type, as has been observed in previous experiments on Nitrogen and Argon (10).

Results and Discussion

Function f in figure 3 shows principal signals at 27.5 $\mu\text{m Hg}$ and 50.2 $\mu\text{m Hg}$. From the separation in density Δn between these two signals we have found using Equation [3] the diameter of Helium to be: 3.0 ± 0.3 Å. This value is close to the van der Waals excluded volume (2.65 Å) estimation (11), although considerably larger than the value corresponding to the heat conductivity measurements (2.30 Å) and to the continuous regime viscosity measurements (1.9 Å) given in the literature (11).

According to Equation [3] the separation in density Δn between consecutive regions of rapid variation of the effective viscosity with density depends inversely on the distance ΔR between concentric shells in relative motion of the viscometer. Therefore, a comparison of the experimental measurements with viscometers differing in ΔR could serve to test the relation $\Delta n \propto 1/\Delta R$. We have done this considering first our present experimental results, and second, the experimental results reported in a previous paper corresponding to a viscometer with $\Delta R = 5.0 \pm 0.1$ cm (4). The separation in density between the main two signals of f in the experimental results reported in (4) which correspond to a viscometer with $\Delta R = 5.0 \pm 0.1$ cm, is $\Delta n = (3.9 \pm 0.6) \times 10^{14}$ molecules/cm³. Introducing this value in Equation [3], we obtain for the atomic cross-section for helium $\sigma = (2.4 \pm 0.3) \times 10^{-15}$ cm², which yield the atomic diameter $d = (2.8 \pm 0.2) \times 10^{-8}$ cm, which is in good agreement with the value presently obtained with a viscometer where $\Delta R = 2.00 \pm 0.05$ cm.

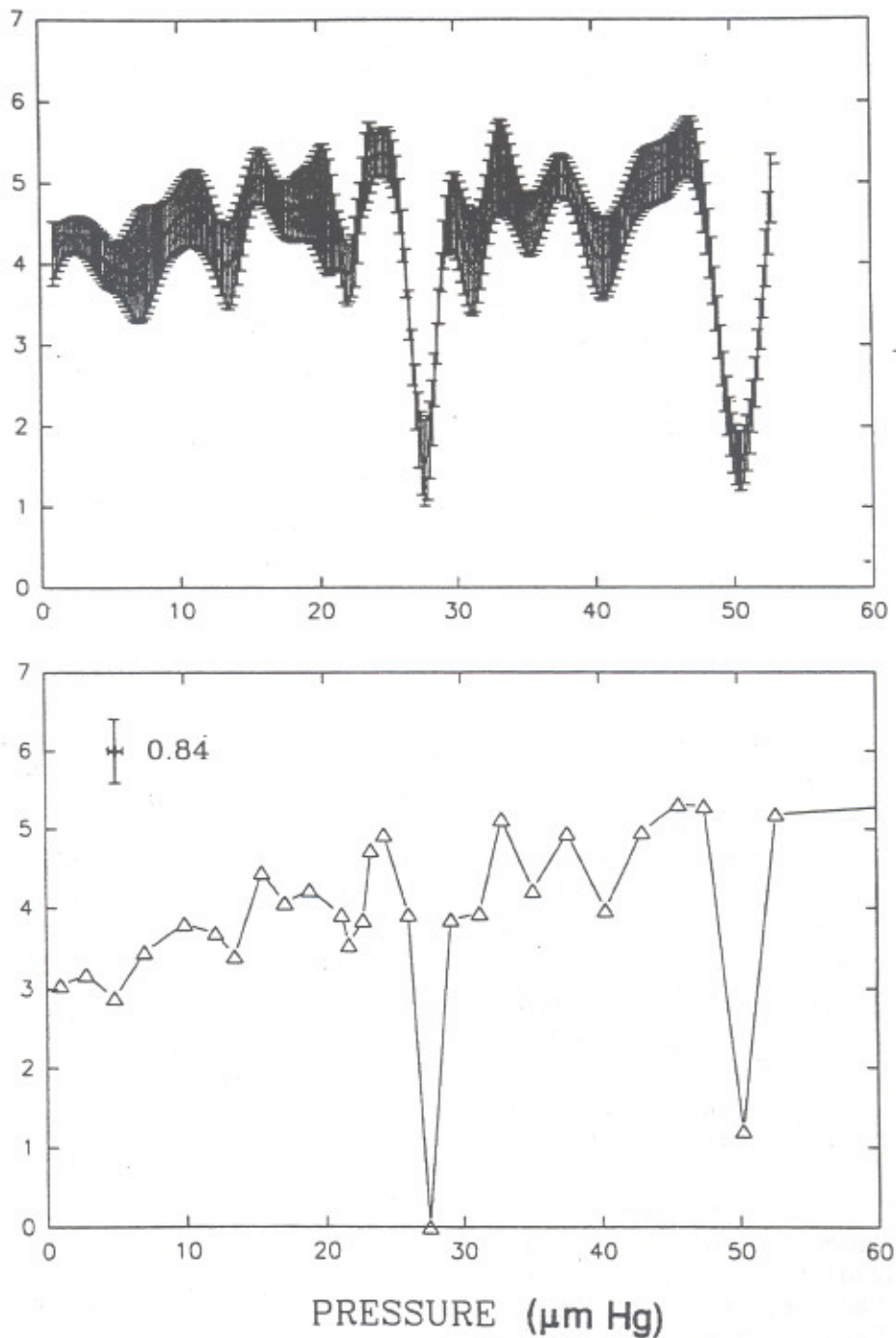


Figure 3. The function $f = -P_{\rho\phi} \Delta R / \eta_0 \Delta v$ vs pressure for a helium gas. The function f is calculated according to Equation (9) from the periods of the torsion pendulum corresponding to different pressures. The distance between surfaces in relative motion of the torsion pendulum is $\Delta R = 2.00 \pm 0.05$ cm. In the upper figure we have represented the error bars associated to every point of the curve.

We have also considered the previous experimental results corresponding to a viscometer in which the internal moving shell is not equidistant from the two fixed surfaces of the apparatus (8). In fact, this viscometer correspond to two ΔR 's distances which are 18.6 ± 0.1 and 4.0 ± 0.1 cm, respectively (8). In order to separate the corresponding two expected "oscillations" of f , the experimental results were analyzed using a Fourier Transform technique. This yielded two values for the atomic diameter of helium with rather large errors: $(2.2 \pm 0.5) \times 10^{-8}$, and $(2.7 \pm 0.7) \times 10^{-8}$ cm, respectively, which taking into account the error bars are still compatible with the two values previously discussed. The second of these values corresponds to $\Delta R = 4.0 \pm 0.1$ cm (8). It is quite close to the values of $(3.0 \pm 0.3) \times 10^{-8}$ and $(2.8 \pm 0.2) \times 10^{-8}$ cm that we have determined above corresponding respectively to $\Delta R = 2.00 \pm 0.05$ cm and $\Delta R = 5.0 \pm 0.1$ cm. Yet, the value $d = (2.2 \pm 0.5) \times 10^{-8}$ cm, which corresponds to $\Delta R = 18.6 \pm 0.1$ cm (8), is appreciably lower than the other two. In spite of the large error involved in this last evaluation of the atomic diameter of helium, this may be an indication that Equation [3] remains valid for variations in ΔR of about 150%, although it may break down for much larger variations. Note that large changes in ΔR imply (according to Equation [3]) large changes in Δn if σ , and so the atomic diameter d , should come out with the same value. Remarkably this is what is experimentally obtained.

Concluding remarks

The consistency of the experimental results reported in this paper, and those reported previously (4,7), with respect to the relation $\Delta n \propto 1/\Delta R$ deduced from Equation [3], is a more stringent experimental test than those presented before for the occurrence of regions of rapid variation of the effective viscosity as a function of density for gases in the transition regime, these regions being separated in density according to the

simple relation in terms of the atomic cross-section of the gas and the separation between moving and fixed walls of the viscometer, Equation [3]. On the other hand, our results bring an additional indication of the importance of the Burnett-type corrections to that recently found in atomistic simulations of a strong shock wave in a hard-sphere gas (3).

Acknowledgements

We thank Oscar Aurenty for technical assistance.

References

1. CHAPMAN S., COWLING T.G. *The mathematical theory of non-uniform gases*, Cambridge University Press, London (England), chaps. 1-4, 1970.
2. KOGAN M.N. *Rarified Gas Dynamics*, Plenum, New York (U.S.A.), chaps. 3 and 5, 1969.
3. SALOMONS E., MARESCHAL M. *Phys Rev Letters* 2 69: 269-272, 1992.
4. MORONTA D., GARCÍA-SUCRE M. *Phys Rev* 2 A18: 756-766, 1978.
5. GARCÍA-SUCRE M., MORONTA D. *Phys Rev* 3 A 26: 1713-1727, 1982.
6. GARCÍA-SUCRE M., ARAQUE-LAMEDA L.A., PARRA R., URBINA-VILLALBA G. *Ciencia* 2(3): 109-116, 1995.
7. GARCÍA-SUCRE M., LAMEDA L., URBINA-VILLALBA G., PARRA R.E. Non-monotonic dependence of transport coefficients of gases on pressure and external thermal gradient in the transition regime. Proceedings of the *Third Caribbean Congress on Fluid Dynamics and the Third Latin-American Symposium on Fluid Mechanics*. Caracas (Venezuela), pp. 1-8, 1995.
8. GARCÍA-SUCRE M., MATA G.J. *Phys Rev* 2 A34: 1591-1594, 1986.
9. JEFFREYS H., JEFFREYS B. *Method of mathematical physics*, Cambridge Uni-

- versity Press, London (England), pp. 240-260, 1972.
10. MORONTA D., GARCÍA-SUCRE M. *Phys Rev* 4 A29: 2263-2264, 1984.
11. Handbook of Chemistry and Physics, 52nd ed., edited by R.C. Weast Chemical Rubber, Cleveland (U.S.A.), pp. F-170, 1971.